Catena 165 (2018) 42–53

Contents lists available at ScienceDirect

Catena

journal homepage: www.elsevier.com/locate/catena

Check dams and afforestation reducing sediment mobilization in active gully systems in the Andean mountains

Pablo Borja[a,b], Armando Molina[c,d], Gerard Govers[d], Veerle Vanacker[b,*]

[a] Facultad de Ciencias Agropecuarias, Universidad de Cuenca, Ecuador
[b] Earth and Life Institute, Georges Lemaître Centre for Earth and Climate Research, Université catholique de Louvain, Louvain-la-Neuve, Belgium
[c] Programa para el Manejo de Agua y Suelo, Facultad de Ingeniería Civil, Universidad de Cuenca, Cuenca, Ecuador
[d] Division of Geography, Department of Earth and Environmental Sciences, KU Leuven, Belgium

ARTICLE INFO

Keywords:
Gully erosion
Soil restoration
Paired catchments
Soil degradation
Sediment yield
Soil and water conservation
Andes
Ecuador

ABSTRACT

Gully erosion is an important process of land degradation in mountainous regions, and is known to be one of the major sediment sources in eroded catchments. Recent studies have suggested that living and dead vegetation can be effective for ecosystem restoration, and large-scale restoration projects have been implemented in the tropical Andes in recent decades. However, few quantitative studies exist on the effectiveness of gully restoration to reduce sediment production and mobilization. In this study, sediment mobilization and transport was studied in five micro-catchments ($< 1\ km^2$) with different soil and water conservation treatments. The techniques that were used for soil and water conservation involve vegetation restoration on the hillslopes and check dams in active gully channels. To characterize the routing of sediment within the micro-catchments, we measured erosion and sediment deposition within the gully channels. Sediment yield was estimated from measurements of sediment accumulation in sediment traps that were constructed at the outlet of the micro-catchments. Flow barriers are shown to be very effective in stabilizing active gully systems in badlands through significant reduction (of > 70%) of the amount of sediment exported from the micro-catchments. The construction of wooden barriers (or so-called check dams) in active gully channels enhances sediment deposition in the gully bed. The latter is strongly dependent on the rainfall intensity, as well as gully channel slope and vegetation cover. The experimental data suggest that there exists a threshold value of rainfall intensity (I_{30}max) of about $23\ mm\ h^{-1}$, above which all sections of the gully system are actively contributing water and sediment to the river network. Also, forestation of active gully systems with rapidly growing exotic species such as *Eucalyptus* has a positive effect on the stabilization and restoration of the badlands, and effectively reduces the sediment export.

1. Introduction

In tropical mountain regions, mass movement and soil erosion by water are the dominant processes that transport soil material downslope (Harden, 2001; Vanacker et al., 2003; Guns and Vanacker, 2013). Water erosion is an important process of land degradation (Poesen et al., 2003), and leads to the development of extensive rill and gully networks and the formation of so-called badlands. When the protective native vegetation cover is removed, the soil becomes rapidly exposed to the effects of erosive rainfall (Inbar and Llerena, 2000; Molina et al., 2007). The rapid generation of surface runoff results in the formation of gullies that further enhances soil degradation by destroying the soil layer and exposing the parent material to the action of water (Harden and Scruggs, 2003). Soil erosion poses important limitations to the development of agriculture, as elevated soil losses have a negative effect on crop productivity (Pimentel et al., 1995; Duan et al., 2016). The off-site effects of soil erosion in tropical mountains are multifold: increasing costs for hydropower installations due to a reduced water storage capacity (Harden, 1993), pollution of water reservoirs and dams that are used to supply drinking water (Harden, 1993; Navarro Hevia et al., 2014), and siltation of irrigation infrastructure.

Data-driven studies show that soil erosion rates in tropical mountain regions have changed significantly in the recent past (Harden, 1993; Harden and Mathews, 2002; Podwojewski et al., 2002; Molina et al., 2007). Changes in land use and land management, modifications of agricultural practices, and climate variability and climate change can alter surface runoff and magnify the intensity of soil erosion processes (Kosmas et al., 1997; Yang et al., 2003; Imeson, 2012). However, a lot of uncertainty exists about future changes in soil erosion and sediment yield (Cadilhac et al., 2017) as quantitative information on sediment

* Corresponding author at: Georges Lemaître Centre for Earth and Climate Research, Université catholique de Louvain, Place L. Pasteur 3, B-1348 Louvain-la-Neuve, Belgium.
E-mail address: veerle.vanacker@uclouvain.be (V. Vanacker).

https://doi.org/10.1016/j.catena.2018.01.013
Received 13 January 2017; Received in revised form 9 January 2018; Accepted 11 January 2018
0341-8162/

production and transport in tropical mountain regions is scarce.

Conservation and restoration of eroded and degraded land is increasing worldwide (De Groot et al., 2013), and assisted vegetation restoration and unassisted vegetation regeneration is gaining momentum (Chazdon, 2008), also in the Tropical Andes (Dehn, 1995; Knoke et al., 2014). Restoration of the protective vegetation cover is an essential component of conservation and restoration projects, as vegetation cover exerts a first-order control over erosion rates (Gyssels et al., 2005; Vanacker et al., 2007b; Molina et al., 2008). An increase in vegetation cover helps to protect the ground surface for raindrop action allowing infiltration and reduction of surface runoff (Bruijnzeel, 2004), to regulate surface hydrology (Thornes, 1990; Kosmas et al., 1997; Bochet et al., 2006) and to reduce rates of water erosion and sediment transport (Rey et al., 2005; Vanacker et al., 2007b; Stokes et al., 2008; Molina et al., 2009; Bellin et al., 2011). Decomposition of organic material leads to an increased input of organic C and N in the soil (Ruiz Sinoga et al., 2012; De Baets et al., 2013), and assists the recovery of the soil functionality (Yüksek and Yüksek, 2011). Additionally, the vegetative cover reinforces the root matrix in the soil mantle and enhances soil cohesion (Bochet et al., 1998; De Baets et al., 2006; Hooke and Sandercock, 2017). A dense and short vegetation cover is an effective way to control water erosion (Sanders, 1988).

Soil and water conservation techniques that combine vegetation protection and restoration with gully restoration can be highly effective in reducing water runoff (Chirino et al., 2006; Descheemaeker et al., 2006; Xu et al., 2008), soil erosion and sediment yield (Rey, 2003; Rey, 2004; Cohen and Rey, 2005; Rey et al., 2005; Zheng, 2006; Burylo et al., 2007; Erktan and Rey, 2013; Marden et al., 2014; Rey and Burylo, 2014). While vegetation restoration on the hillslopes aims to reduce soil erosion and surface runoff by restoring the soil functions on-site, the construction of check dams in the gully channel aims to reduce transfer of surface runoff and sediments downstream (Xiang-Zhou et al., 2004; Boix-Fayos et al., 2008; Molina et al., 2009).

There is a growing number of studies that highlight the effectiveness of soil and water conservation techniques for conservation and restoration of eroded land. In the Ethiopian Highlands, an integrated landscape restoration programme included the implementation of terrace agriculture, construction of check dams and gabions in stream and gully channels and establishment of exclosures or set-aside areas (Descheemaeker et al., 2006; Haregeweyn et al., 2015). Taye et al. (2015) showed that the soil and water conservation measures are more effective in reducing soil loss than runoff, and that the effectiveness of many structures quickly declines over time. In the dry valley of Minjiang River, SW China, three different plant species were tested for their effectiveness to reduce water runoff and soil loss: Xu et al. (2008) report that plant characteristics such as leaf area, canopy density and height control the effectiveness of the vegetation to improve soil properties and reduce runoff and soil loss. The position and distribution of vegetation patches is crucial to understand sediment mobilization and transport within eroded catchments (Rey, 2003). Rey (2004) and Rey and Burylo (2014) demonstrated that vegetation barriers are very effective to trap sediment, as a vegetation barrier covering only 20% of a 500 m^2 plot can be sufficient to trap all the sediments eroded above it. Molina et al. (2009) showed that the presence of a dense vegetation cover in gully floors results in significantly lower sediment transfer: the deposition of eroded sediments in the gully bed can represent > 25% of the volume of the sediment generated by erosion processes within the catchment. This was also shown by Navarro Hevia et al. (2014) for badlands in Spain where check dams and restored forest buffers effectively reduced the sediment yield in the Carrion River by almost three orders of magnitude.

In the Ecuadorian Andes, the formation of gullies dates back to at least the 1960s (Vanacker et al., 2003). The majority of erosion research focused on rill and inter-rill erosion based on plot scale experiments. For abandoned land in southern Andean Ecuador, Harden (1993, 2001) measured sediment detachment rates up to 3.7 g mm^{-1} with a portable rainfall simulator, and reported erosion rates up to 95 t ha^{-1} yr^{-1} based on non-published technical reports of plot erosion measurements. She reported higher erosion rates (up to 836 t ha^{-1} yr^{-1}) for northern Andean Ecuador (Harden, 1988). An important issue in erosion research is the spatial extent of the study area, as erosion and deposition processes are scale-dependent (Garcia-Ruiz et al., 2015). Extrapolation of erosion data measured at the plot scale to the catchment scale has proved problematic, and often results in large uncertainty on sediment yield estimates (Vanacker et al., 2007b). Molina et al. (2008) pointed out that small hydrological units such as micro-catchments (0.1–10 km^2) are interesting environments to study erosion processes in mountain areas, given the large spatial heterogeneity in climate, topography, soils and vegetation cover that exists over short distances. Analyzing erosion processes at the spatial scale of small hydrological units allows one to limit the existing variability in climate, lithology and topography to a minimum, and isolate the effects of e.g. vegetation cover or land use on erosion rates.

This paper provides new data on sediment dynamics and its controlling factors for the tropical Andes. In contrast to earlier work (Harden, 1993; Molina et al., 2008; Molina et al., 2012), this study focuses on highly disturbed badland areas that are important sources of sediment in the central Andean valleys. Through a quantitative assessment of sediment transport, deposition and export in five micro-catchments (< 1 km^2), the paper evaluates sediment dynamics in gully systems. The five micro-catchments differ in the implementation of soil and water conservation measures, with one micro-catchment treated with *Eucalyptus globulus* reforestation, two with unassisted vegetation regeneration and construction of check dams for gully stabilization, and two non-treated or reference micro-catchments. An erosion monitoring program implemented in 2010 provided detailed information on sediment transport, deposition and export at the treated and reference sites.

1.1. Study area

The study area, the Loreto catchment, is located in the southern Ecuadorian Andes at 23 km south of Cuenca city (Fig. 1). The rainfall regime in the Cuenca area is bimodal with two rainy seasons, registering between 600 and 1000 mm of yearly rainfall (Celleri et al., 2007; Mora and Willems, 2012). In the study area, an average rainfall of 913 mm yr^{-1} was measured (01/02/2011–30/08/2014). Soils developed on highly weathered volcanic and sedimentary rocks. The shallow soils are generally clay-rich with over 50% of the soil material consisting of clay minerals. More than half (in total clays) of these clay minerals consist of 2:1 dioctahedral clays, mainly smectites and mixed-layered minerals containing smectite (Molina et al., 2007). The major soil types in the valleys are Vertic Luvisols, Vertic Cambisols, and Eutric Cambisols. On the slopes, Dystric Leptosols and Dystric Regosols are found: these thin soils are characterized by a low organic matter content (IUSS Working Group WRB, 2015). The shallow and clay-rich soils have low water holding capacity, and are poorly drained (Molina et al., 2007).

The landscape is a patchwork of small agricultural fields, remnants of secondary forests, exotic tree plantations, badlands, residential areas and infrastructure. Crops are typically produced on the more fertile soils in the valleys while extensive cattle raising extends to the steep slopes. Overgrazing and intensive cultivation has led to severe land degradation, with the development of extensive gully systems and so-called badland areas (Molina et al., 2008). As a result, highly degraded and eroded land has temporarily or permanently been abandoned for agriculture and extensive grazing. Reforestation with quickly growing exotic species such as *Eucalyptus globulus* and *Pinus radiata* became a viable land use alternative in the late 1970s due to the growing demand of firewood and timber. After abandonment, woody and shrubby plant species started to colonize spontaneously the land.

Recent work by Molina et al. (2008) in southern Ecuadorian Andes has reported catchment-wide erosion rates varying between 0.26 and

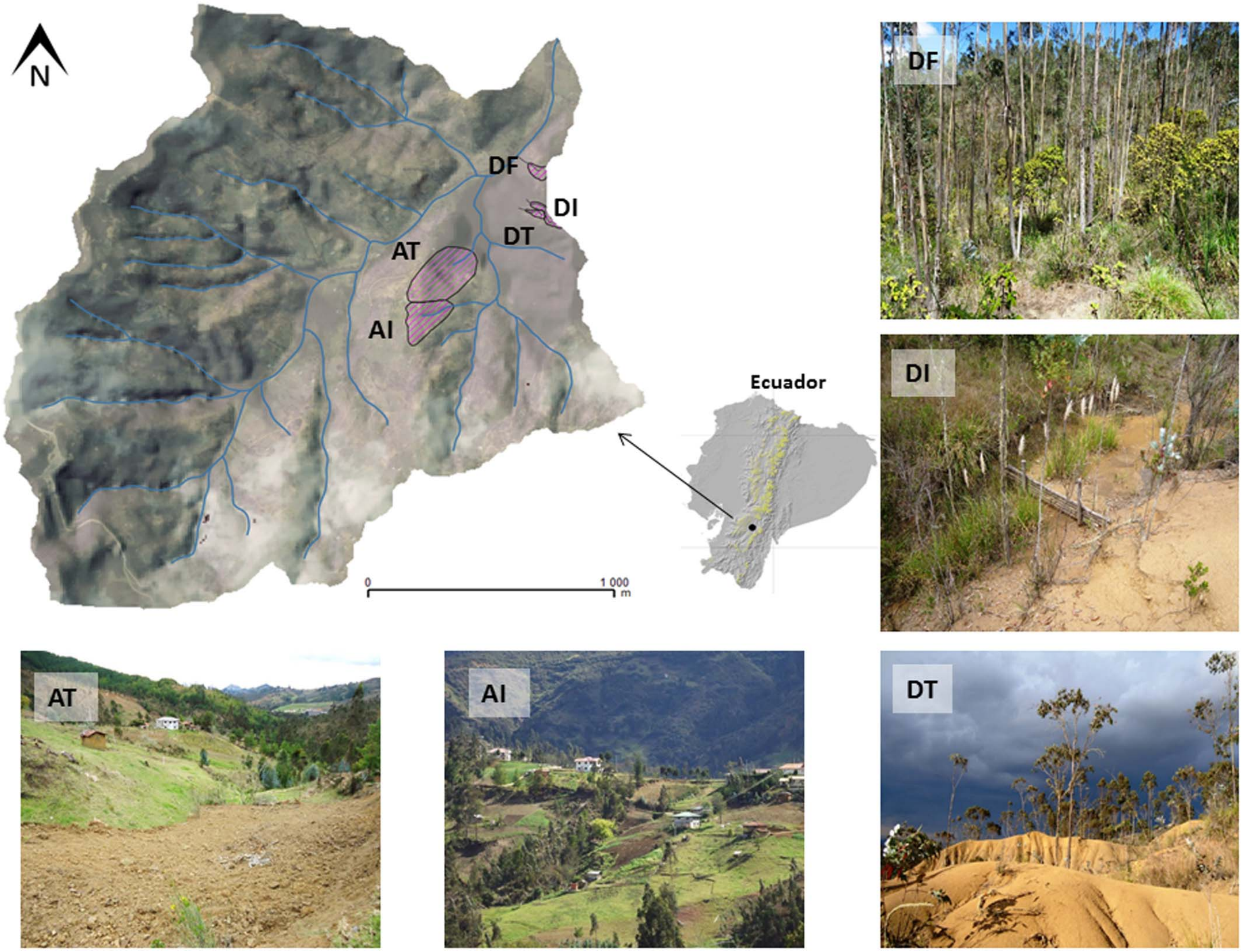

Fig. 1. Location of the study area in the Southern Ecuadorian Andes. The five pictures illustrate the vegetation cover of the five micro-catchments (DT, DI, DF, AI, AT), and their main characteristics are given in Table 1. Topographic information is derived from a 10 m DTM, and a Quickbird satellite image of 2008 (Google earth V 6.2, 2012) is given as background.

Table 1
Main characteristics of the five experimental micro-catchments, with overview of the main gully characteristics and soil and water conservation (SWC) treatments. Afforestation was realized by UMACPA in the 1980s, and 47 check dams were constructed in 2010 by the ARES PRD research team.

	ID	Land cover	SWC treatment	Surface ha	L m	S $m\,m^{-1}$
Reference micro-catchments in…						
- Eroded land	DT	75% barren land 24% shrubs 1% forest	NA	0.20	84	0.27
- Agricultural land	AT	64% grassland 18% arable land 14% barren land 4% forest	NA	4.7	340	0.21
Treated micro-catchments in…						
- Eroded land	DI	59% barren land 27% forest 14% shrubs	12 check dams in gully channel Plantation of *Eucalyptus globulus* in 27% of area (headwaters)	0.42	179	0.20
- Forested land	DF	61% forest 39% barren land	Plantation of *Eucalyptus globulus* in 61% of area	0.42	95	0.42
- Agricultural land	AI	49% arable land 19% grassland 17% shrubs 8% barren land 7% forest	35 check dams in gully channel Plantation of *Eucalyptus globulus* in 7% of area (headwaters)	2.4	209	0.19

Table 2
Sediment budget for the five micro-catchments. The sediment yield ($t\,ha^{-1}\,yr^{-1}$) is determined at the outlet of the micro-catchments, and the sediment deposition in the gully channels ($t\,ha^{-1}\,yr^{-1}$) is based on the measurement of sedimentary wedges behind check dams. The total amount of sediment ($t\,ha^{-1}\,yr^{-1}$) mobilized in the micro-catchments is the sum of the two latter values, and is also expressed as the catchment-wide erosion rate ($mm\,yr^{-1}$). For the treated micro-catchments, the values between brackets represent the net erosion rate obtained from the data on sediment export. Note that these values correspond to minimum estimates, as no correction is made for the trap efficiency of the structures.

	Sediment yield ($t\,ha^{-1}\,yr^{-1}$)	Sediment deposition ($t\,ha^{-1}\,yr^{-1}$)	Total ($t\,ha^{-1}\,yr^{-1}$)	Erosion rate ($mm\,yr^{-1}$)
DT	89.1		89.1	6.14
DI	24.3	81.5	105.9	7.30 (1.68)
DF	1.18		1.18	0.08
AI	2.49	15.7	18.2	1.26 (0.17)
AT	0.23		0.23	0.02

$151\,t\,ha^{-1}\,yr^{-1}$, largely as a result of variations in vegetation cover, lithology and topography. The Loreto river, a tributary of the Jadan river, was selected for this study: soil erosion is evident, and catchment-wide erosion rates of $75.8\,t\,ha^{-1}\,yr^{-1}$ were measured in this area (Molina et al., 2008; Fig. 1). Within the Loreto catchment, five experimental sites (corresponding to hydrological units or micro-catchments) are selected with similar topographic, climatic, and geological setting. The surface area of the elongated micro-catchments ranges between 0.20 and 4.7 ha (Table 1). Two experimental sites are located in agricultural land, and three sites in highly eroded lands or so-called badlands (Fig. 1). The dense network of rills and gullies in the badlands is directly connected to the fluvial system, and influences the hydrological response of the Loreto and Jadan River system. The time of formation of the badland topography is not known at present, and most of them pre-date the first aerial photographs (1962) of the region. The ephemeral and permanent gullies in the five micro-catchments are V-shaped, with a gully depth ranging between 0.5 and 4.0 m, a total channel length between 80 and 350 m, and an average slope gradient between 19 and 42% (Table 1). We refer to Molina et al. (2009) for a detailed description of the gully characteristics.

Soil and water conservation (SWC) measures were applied in three of the five micro-catchments, the so-called "treated" micro-catchments (Table 2, Fig. 1). Two micro-catchments are not treated, respectively in the agricultural and eroded land, and serve as "reference" sites. In this study, we refer to the micro-catchments in agricultural land as "AT" (non-treated site) and "AI" (treated site), and to the ones in eroded land or badlands as "DT" (non-treated site), "DI" (treated site) and "DF" (treated site with forest plantation). It is important to note that the micro-catchments in the agricultural land (AI, AT) and eroded land (DI, DF, and DT) had a very similar land use and vegetation cover in the 1960s (Molina et al., 2012). As such, the differences in soil and sediment dynamics that are observed are reflecting the impact of the soil and water conservation schemes.

2. Materials and methods

In the scope of a research program (2009–2014) at the University of Cuenca (Ecuador), an erosion monitoring program was designed in 2009, and implemented in the field from 2010 onwards. Two tipping bucket rain gauges (Davis Rain Collector) were installed to monitor rainfall during the period 01/02/2011–30/08/2014. The topographic and vegetation survey started in 2011, and continued in 2012 and 2014. The gully restoration project was implemented in the DI and AI micro-catchments in July 2010, and sediment accumulated behind the 45 check dams was measured from 01/07/2011 (start of sediment deposition behind check dams) until 30/05/2012 (sedimentary wedges filled till maximum storage capacity; Fig. 4). The sediment accumulation in the traps at the outlet of the micro-catchments was measured from 01/07/2011 until 30/07/2014 (Fig. 7).

2.1. Characterization of the micro-catchments

Digital topographical maps (1:10,000) were used for the delimitation of the micro-catchments. The dense network of gullies was mapped in the field using a handheld GPS with a horizontal accuracy of 5 m. Based on the digital topography, maps of local hillslope gradient and orientation were made in ArcGIS 10.3. A vegetation map (1:10,000) was made based on field observations of vegetation type and density. Polygons with homogeneous vegetation cover were identified in the field, and mapped using a handheld GPS. The following vegetation classes were identified: grasses, forest, scrubs, shrubs, arable land and barren land (Fig. 1).

2.2. Soil and water conservation treatments

Erosion mitigation in the wider area was largely an initiative taken by the former Instituto Nacional de Electrificación (INECEL) and the Unidad de Manejo de la Cuenca del Río Paute (UMACPA) in the 1980s and 1990s to restore highly eroded catchments and reduce sediment transport in the Paute river system. The restoration programs of UMACPA consisted in the construction of check dams in small tributaries to adjust the gradient of the gully channels, reduce the erosive power of the river and reduced the sediment export to the Paute River. It also included vegetation restoration through plantations of *Pinus* and *Eucalyptus* trees on eroded land. The DF micro-catchment corresponds to an area that was reforested with *Eucalyptus globulus* in the 1980s, and > 60% of its surface area is covered by forest. Trees were planted at relatively low density, which permitted the establishment of herbaceous and shrub undercover through natural regeneration of native plant species (Fig. 1). In the remaining micro-catchments (DT, DI, AI and AT), the forest cover is generally low and up to respectively 1%, 27%, 7% and 4% (Table 1).

The gully restoration project is complementary with the vegetation restoration project of UMACPA that initiated in the area in the 1980s and 1990s, and implemented physical structures in the gully channels of the DI and AI micro-catchments. Table 1 gives an overview of the different treatments. The small vegetative barriers were assembled using 15 cm-diameter wooden poles, and were constructed perpendicular to the flow direction of the ephemeral streams. After hammering two to three strong wooden poles in the base of the gully floor, wooden stakes (and in a few cases, recycled tires) were piled up behind the line of poles. The poles and stakes were fixed by means of metal wire and nails so that the structure is firm and stable (Fig. 2). The structures are typically 1 to 3 m wide and 0.35 to 0.8 m high. The distance between consecutive check dams is 1 to 22 m. A total of 47 check dams were constructed: 12 and 35 check dams in the DI and AI micro-catchment respectively (Table 1, Fig. 2). Their location is not random, and they are often located downstream of a confluence of two or more gully channels in order to keep the number of check dams at a minimum. During the duration of the study, seven of a total of 47 check dams were damaged and two were completely destroyed. Destruction was due to vandalism and theft of wood. In the agricultural micro-catchment (AI), the majority of the damaged check dams were quickly repaired. In the micro-catchment in eroded land (DI), two check dams were completely destroyed and not repaired.

2.3. Monitoring of sediment transfer and export

Our method for calculating sediment deposition in the gully floor is based on Sougnez et al. (2011), as Ramos-Diez et al. (2016) have shown the robustness of this field method. The depth and width of multiple sedimentary wedge sections were measured on a weekly basis to estimate the total volume S_V (m^3) of sediment retained using the following

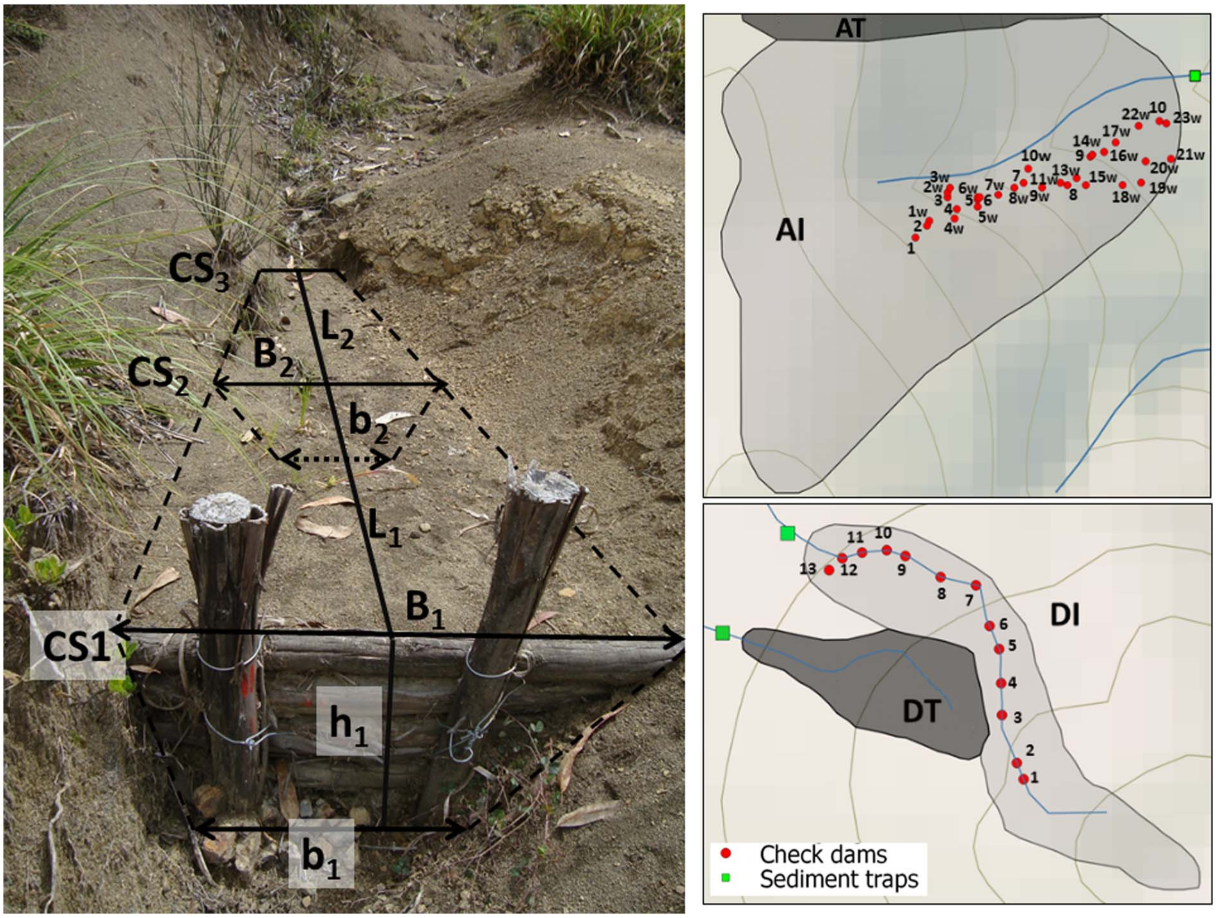

Fig. 2. Overview of the check dams in the AI and DI micro-catchments. Left panel: sedimentary wedge behind wooden check dam with indication of the field measurements that were realized for the determination of its sediment volume. Right panels: Location of the check dams in the AI (upper right) and DI (lower right) micro-catchments.

equations (Fig. 2):

$$S_V = \sum_{i=1}^{n} \left(\frac{CS_i + CS_{i+1}}{2} \right) \cdot L_i \quad (1)$$

where CS_i is cross-sectional area (m^2) of the ith cross-section, and L_i (m) is the length of the wedge between its ith and i + 1th sections (Fig. 2). The cross-sectional area CS_i is determined as:

$$CS_i = \frac{(B_i + b_i)}{2} \cdot h_i \quad (2)$$

with h_i is the depth of the sediment deposit (m), and B_i and b_i are respectively the top and bottom width of the sedimentary wedge (m).

At the outlet of every micro-catchment (DI, DT, DF, AT and AI), a sediment trap was constructed to estimate the sediment yield of the catchment. All traps consist in a pit of 1 × 1 × 0.5 m that was dug in the main gully channel. The base of the trap was covered with concrete and the walls were reinforced with wooden poles till a height of 0.5 m. The material accumulated in the traps was measured at weekly basis. Occasionally when the trap was completely filled with sediment, sedimentation occurred in the gully channel downstream of the sediment trap. On these occasions, the total volume of sediment deposited was determined by summing the volume of sediment accumulated in the trap and the sediment deposited in the channel. The latter was determined based on linear measurements using surveyor's tapes in the field.

In our results, the sediment accumulation in a given structure, S_V, is expressed in m^3 of sediment accumulation. Values of S_V were divided by the maximum storage capacity of the structure to obtain the relative infilling S_{VE} ($m^3\,m^{-3}$) which allows comparison in filling rates between check dams of different size. The volume of sediment that accumulates in the sediment traps is expressed in m^3 per surface area of its drainage basin (ha). In order to convert the sediment volumes into sediment mass, the bulk density was calculated from 104 sediment samples taken in metallic cylinders of 100 cm^3. To get a first estimate of sediment fluxes ($t\,ha^{-1}\,yr^{-1}$) in the micro-catchments, the sediment masses (t) were divided by the time period of observations (yr) and the contributing drainage area (ha).

2.4. Monitoring rainfall amount

The rain gauges (P-Lo1, and P-Lo2) are situated in the Loreto catchment, in proximity of barren and arable lands. The resolution of the rain gauges is 0.2 mm and both gauges were installed at a height of 1.8 m. The rain gauge P-Lo1 (barren land) was used for estimating rainfall amount and intensity, while P-Lo2 (agricultural land) was used only to complete data gaps during short periods when P-Lo1 was damaged. The two rain gauges are located at similar altitude and at < 1 km distance from each other. Rainfall data was aggregated to an hourly and daily temporal resolution and periods without data were filled with information of the second rain gauge (P-Lo2). There is a gap in the rainfall series of 4 days during the period 22/03/2014–26/03/2014 and 28 days for the period 17/07/2014–14/08/2014. The maximum rainfall intensity during 30 min, I_{30max} ($mm\,h^{-1}$), was calculated for each runoff event.

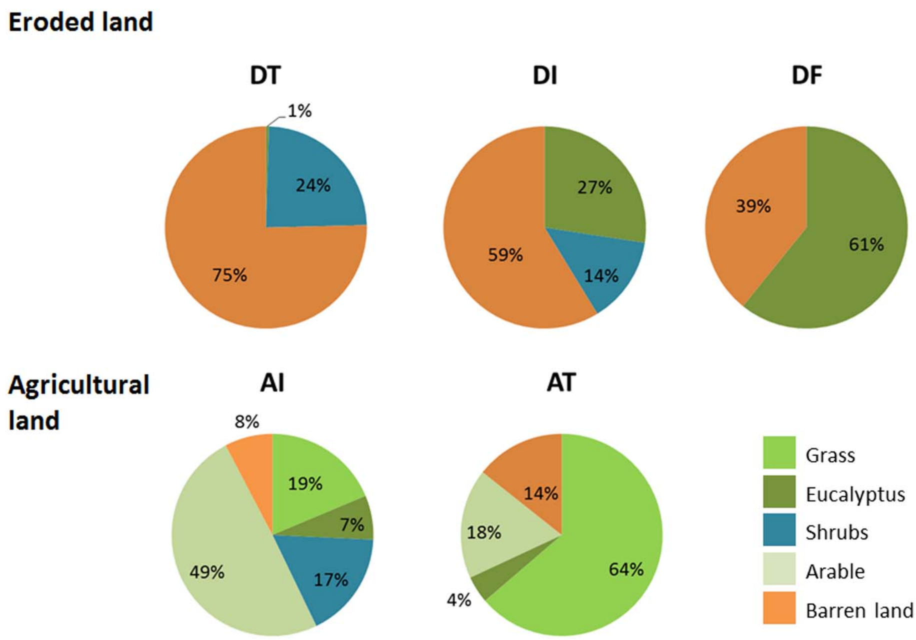

Fig. 3. Vegetation cover for the five micro-catchments in eroded (DT, DI and DF) and agricultural land (AI and AT). We refer to Fig. 1 for the location of the micro-catchments.

3. Results

3.1. Vegetation cover of the five micro-catchments

In the two eroded catchments, barren land represents 59% and 75% of the surface area of respectively the DI and DT catchments (Fig. 3). The DI catchment is slightly larger than the DT catchment, and has *Eucalyptus globulus* plantations with understory of shrubs and grasses in its headwaters. The DF micro-catchment is covered by *Eucalyptus globulus* forest in the middle and lower part of the basin (61% of its surface area), and patches of barren land in its headwaters (39% of surface). The deep and wide root systems of the *Eucalyptus* trees anchor the soil and weathered bedrock. The forest plantations have a low density: tree trunks are randomly distributed with a mean distance between the trunks of > 4 to 5 m. In the badlands, the growth of trees is very irregular with a stem density lower than $3/100\,m^2$. A lush understory of herbs and shrubs is present, with dominance of zig-zal (*Cortaderia rudiuscula*), retama (*Spartium junceum*) and chilca (*Baccharis polyantha*) shrub species, and kikuyu (*Pennisetum clandestinum*), grama (*Holcus lanatus*), pajilla (*Festuca megalura*) and grama de la virgen (*Cynodon dactylon*) grasses and weeds that spontaneously colonize abandoned land.

The agricultural catchments (AT and AI) are mainly covered by grassland (respectively 64% and 19% of surface area) and cropland (respectively 18% and 50% of surface area). Although their total surface of agricultural land is rather similar (respectively 82% and 69%), the non-treated site (AT) clearly has a larger proportion of grasslands compared to the treated site (AI). The dominant crops are *Zea mays*, *Pisum sativum*, *Phaseolus vulgaris*, and *Vicia phaba*. In the grasslands, *Pennisetum clandestinum* and *Medicago sativa* are the dominant species.

3.2. Rainfall characteristics

Rainfall data covers almost four years (Jan 2011 till Aug 2014). Rainfall amounts registered in the two gauges are very similar, at daily time step. Small differences exist at hourly time step for storm events. The summer months of July, August and September are typically dry, and the wet season covers the period October to May (Fig. 4). The frequency analysis shows that few events (8% of all rainfall events) have an intensity that is higher than $10\,mm\,h^{-1}$. Rainfall events are mostly individual rain events bound by a period of no rainfall. The maximum rainfall intensity registered was $80.8\,mm\,h^{-1}$, and had a duration of 30 min. This event has a recurrence time of 38 years, based on the meteorological data of PROMAS at the University of Cuenca. For the Cuenca meteorological station (located at 23 km distance from Loreto), Harden (1993) reported only 3 to 4 events per year with an intensity of $> 27\,mm\,h^{-1}$.

3.3. Sediment transfer in gully systems

Grain size analyses show that the sediment accumulated behind the wooden check dams and the topsoil material are dominated by small particles, with the silt as the most abundant particle. From five sediment samples, the sand, silt and clay content was estimated at respectively 17, 53 and 30% (silty clay loam). Topsoil from the eroding slopes was classified as silt loam with an average sand, silt and clay percentage of respectively 23, 55 and 22% (n = 10). This indicates that the check dams are efficient in trapping the eroded material, as there are only slight differences in grain size between the sources of erosion and the deposition sites. Our data are not corrected for the trapping efficiency of the structures, and sediment fluxes should be interpreted accordingly.

Fig. 4 shows the filling history of the 45 check dams for the first 500 days after the construction of the flow barriers. The data show that the infilling of check dams in the AI and DI micro-catchments occurs simultaneously during or immediately following rainfall events. This confirms that the data are consistent, and that sediment mobilization within the gully systems is responding effectively to a common trigger, i.e. erosive rainfall. The first 280 days after check dam construction correspond to a prolonged dry season in the region, and sediment deposition behind all 45 check dams was negligible. At the beginning of the rainy season of 2011, the erosive rainfall event of 5 October with an intensity of $> 30\,mm\,h^{-1}$ led to a first and significant increment in sediment deposition in the gully channels of the DI and AI micro-catchments (Fig. 4). In the forty days following this event (between 280 and 320 days after check dam construction), about 87% of the check dams were filled to their maximum storage capacity ($S_{VE} = 1$).

To understand the spatial variation in sediment deposition along the gully channel, we analyze the strength of the relation between rainfall intensity and sediment deposition in a given check dam as a function of its location within the micro-catchment. Based on data for 24 erosive rainfall events, the correlation coefficient between the rainfall intensity

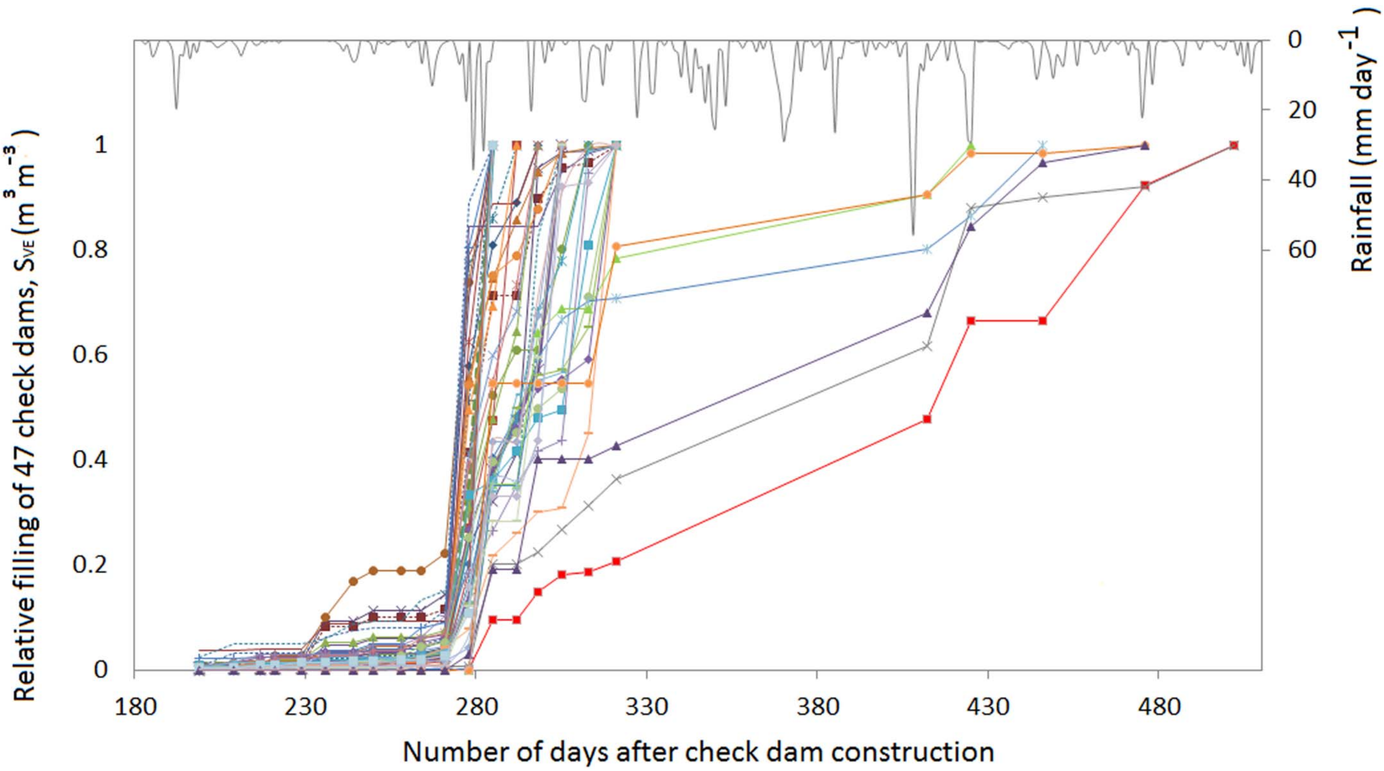

Fig. 4. Filling history of the 45 check dams in the DI and AI micro-catchments covering the period 01/07/2011–30/05/2012. The S_{VE} values ($m^3 m^{-3}$) give the ratio of the sediment deposited to the maximum storage capacity of the structures. A value of $S_{VE} = 1$ means that the maximum storage capacity is reached. Daily total rainfall (aggregated from hourly rainfall data) is plotted on the second Y-axis.

(I_{30max}) and sediment deposition in the check dam (S_V) is calculated. Fig. 5 plots the correlation coefficients as a function of the distance between the check dam and the outlet of the DI and AI micro-catchments. In the DI micro-catchment, the upper part of the catchment is highly responsive to rainfall events, and check dams that are distant from the outlet show a very good correlation between the amount of sediment accumulation and the I_{30max} of the preceding rainfall event (Fig. 5, left-hand panel). Sediment accumulation in the most upstream dams is the direct result of sediment mobilization during rainfall runoff events in the most upstream part of the drainage basin. The relation between rainfall intensity and sediment deposition is less pronounced in the middle and lower part of the DI micro-catchment. Along the gully channel, the implementation of check dams alters the local hydrology through infiltration of runoff water in the sedimentary wedges and reduction of runoff and sediment transfer. Besides, the morphology of the gully system is often complex in its downstream part where runoff can be the result of concentrated runoff from several slopes due to the effect of flow convergence (Verstraeten et al., 2006). In the AI micro-catchment (Fig. 5, right-hand panel), the relation between the rainfall intensity and sediment deposition shows no major change as function of the spatial location of the check dam along the gully system. The fact that the hydrology of the agricultural catchment is highly altered by road and irrigation infrastructure might have altered the flow connectivity of the gully network.

3.4. Sediment yield of the micro-catchments

Based on the sediment accumulation rates in the traps, a first

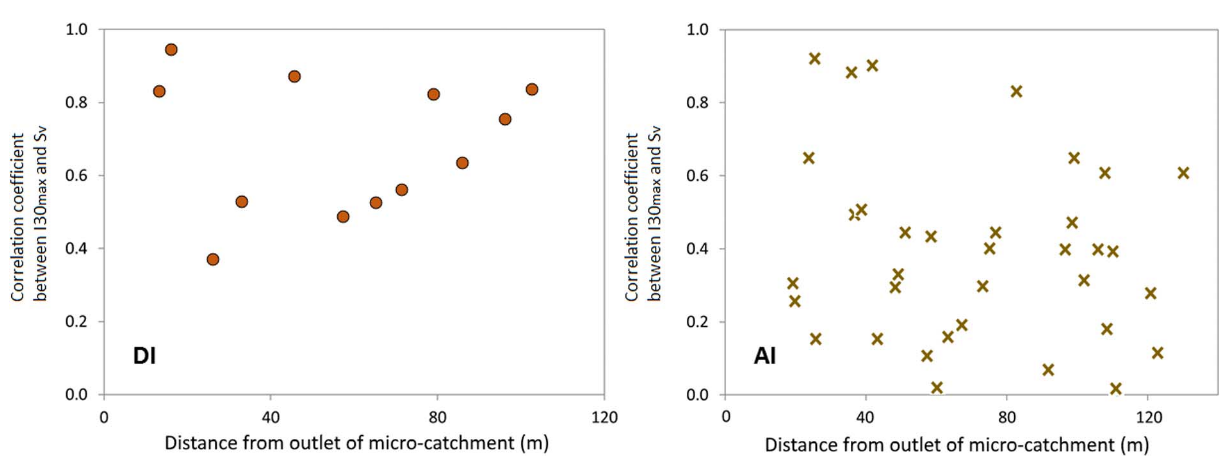

Fig. 5. Dependency of sediment accumulation in the check dams on rainfall intensity. The data show the correlation coefficients between the amount of sediment, S_v, accumulated behind a given check dam and the I_{30max} of the rainfall event that triggered the sediment mobilization as a function of the location of the check dam in the gully channel. The latter is plotted as the distance between the check dam and the outlet of the micro-catchment. The left panel shows results for DI, and the right panel for AI micro-catchment.

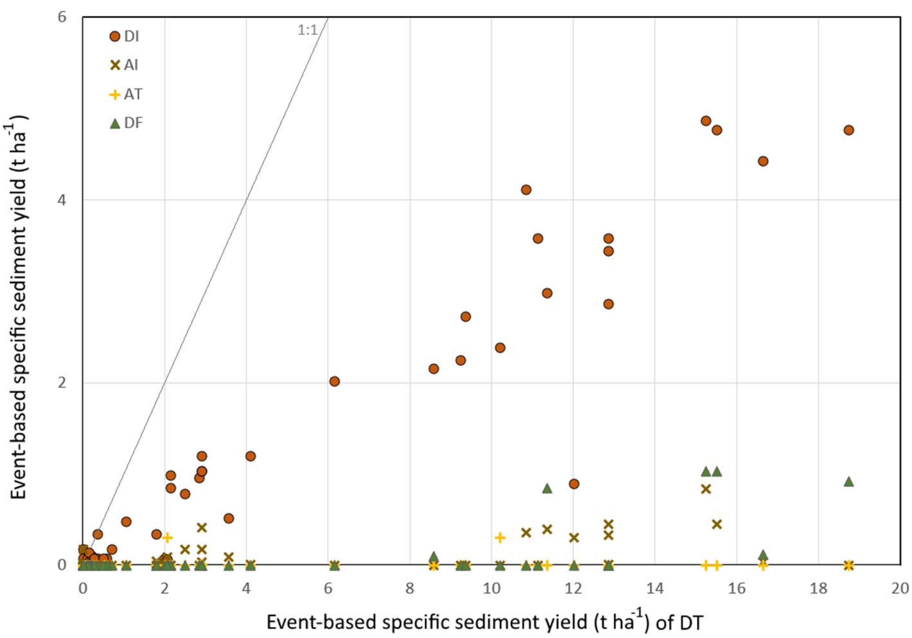

Fig. 6. Event-based specific sediment yields of four micro-catchments. The scatterplot shows the relation between the specific sediment yield in a given micro-catchment (DI, AI and AT; Y-axis) and the DT micro-catchment (X-axis). The treated sites in eroded land (DI and DF), and agricultural land (AI and AT) have lower sediment yield compared to the reference micro-catchment DT.

estimate of the specific sediment yield can be made for the five micro-catchments (Table 2). We used a measured average bulk density of the sediment of 1.43 ± 0.12 g cm^{-3}. The event-based sediment yield data of the five micro-catchments are strongly correlated, with a Pearson correlation coefficient of 0.93 for the sediment yield of the treated (DI) and non-treated (DT) micro-catchments (Fig. 6). Besides high internal consistency of the datasets, this also shows that the micro-catchments are responding to the same trigger, i.e. high intensity rainfall events.

The specific sediment yield of the five micro-catchments differs by two orders of magnitude (Table 2). The specific sediment yield is highest for the reference site in the eroded land (DT) with a value of 89.1 t ha^{-1} yr^{-1}. This roughly corresponds to a net erosion rate of 6.14 mm yr^{-1} for the catchment affected by active gully erosion (Table 2). In the two micro-catchments in eroded land where soil and water conservation measures were implemented, a value of 24.34 t ha^{-1} yr^{-1} was established for the DI micro-catchment, and 1.18 t ha^{-1} yr^{-1} for the DF micro-catchment restored with forest plantations. This corresponds to a net erosion rate of respectively 1.68 and 0.08 mm yr^{-1}. The two micro-catchments in agricultural land, AT and AI, have much lower specific sediment yields of respectively 0.23 and 2.49 t ha^{-1} yr^{-1}, corresponding to erosion rates of approximately 0.02 and 0.17 mm yr^{-1} (Table 2). For the AT micro-catchment, the sediment yield was very low during the period of observation; and only two heavy rainfall events triggered sediment transport in the gully channel.

The sediment yield is strongly associated with the rainfall pattern. The specific sediment yield of the five micro-catchments is highest during and shortly after high-intensity rainfall events. In Fig. 7, the sediment yields of the DT, DI, DF, and AI micro-catchments are plotted as a function of time. In the forested micro-catchment, only 6 rainfall events triggered sediment mobilization in the gully channel and sediment accumulation in the trap (Fig. 7), illustrating the effectiveness of *Eucalyptus globulus* in reducing sediment production, mobilization and export. In the plantation forest, there exists a well-established ground vegetation of herbs and shrubs that protects the soil surface effectively. Although the forest covers only 61% of the catchment area, it has a large impact on the reduction of sediment production and mobilization. Results from AT are not shown in Fig. 7 as only two events led to (very low amounts of) sediment accumulation in the traps.

The sediment yield data show that the sediment export highly depends on the sediment production and mobilization in the gully channels. Our data do not show an increase in sediment yield after filling of the flow barriers (Fig. 7): even when all 45 check dams are filled to about 90 to 100% of their capacity (i.e. 500 days after their construction), the sediment yield of the treated micro-catchments (DI and AI) stays consistently low. To analyze the effect of the check dam filling on the sediment yield of the treated catchments, we analyzed the relationship between the event-based specific sediment yield of DI and DT (m^3 ha^{-1}) before and after the fillings of the flow barriers. The R^2 values of the regression analysis are respectively 0.97 and 0.91 for the periods before and after the infilling of the check dams suggesting that the physical structures have a lasting impact on sediment mobilization within the gully channels. This can also be observed in Fig. 6 where the relation between the event-based specific sediment yield in the DT and DI micro-catchments stays constant over the period of observations.

3.5. Effectiveness of check dams to reduce sediment export

By comparing the micro-catchments with/without soil and water conservation measures (AT vs. AI, DT and DF vs. DI micro-catchments), it is possible to quantify the effectiveness of the treatments to reduce the sediment yield of the gully systems. Fig. 8 gives the simplified sediment budget for the five micro-catchments, where the sediment storage within the gully system is derived from the data on sediment deposition behind the check dams and the sediment export from the data on specific sediment yield (Table 2). For the micro-catchments in eroded land, the dominant erosion process is gully erosion. The reference site DT has a specific sediment yield of 89.1 t ha^{-1} yr^{-1}, representative for the overall erosion rate of non-treated upstream catchments. The specific sediment yield of the DT catchment is – on average – 75 and 3.7 times higher than the sediment yield in the DF and DI catchment, illustrating the efficiency of the soil and water conservation measures to reduce sediment export (Table 2, Fig. 8). The implementation of check dams in the active gully channel of DI led to a net deposition of 34.23 metric tons in the gully channel, corresponding to a net deposition rate of 81.5 t ha^{-1} yr^{-1}. Our data suggest that only 23% of the sediment mobilized in the eroded catchment reaches the outlet of the DI catchment (Fig. 8). In the agricultural land, the specific sediment yield is consistently lower than in the eroded land, i.e. 0.23 t ha^{-1} yr^{-1} for AT compared to 89.1 t ha^{-1} yr^{-1} for DT (Table 2, Fig. 8).

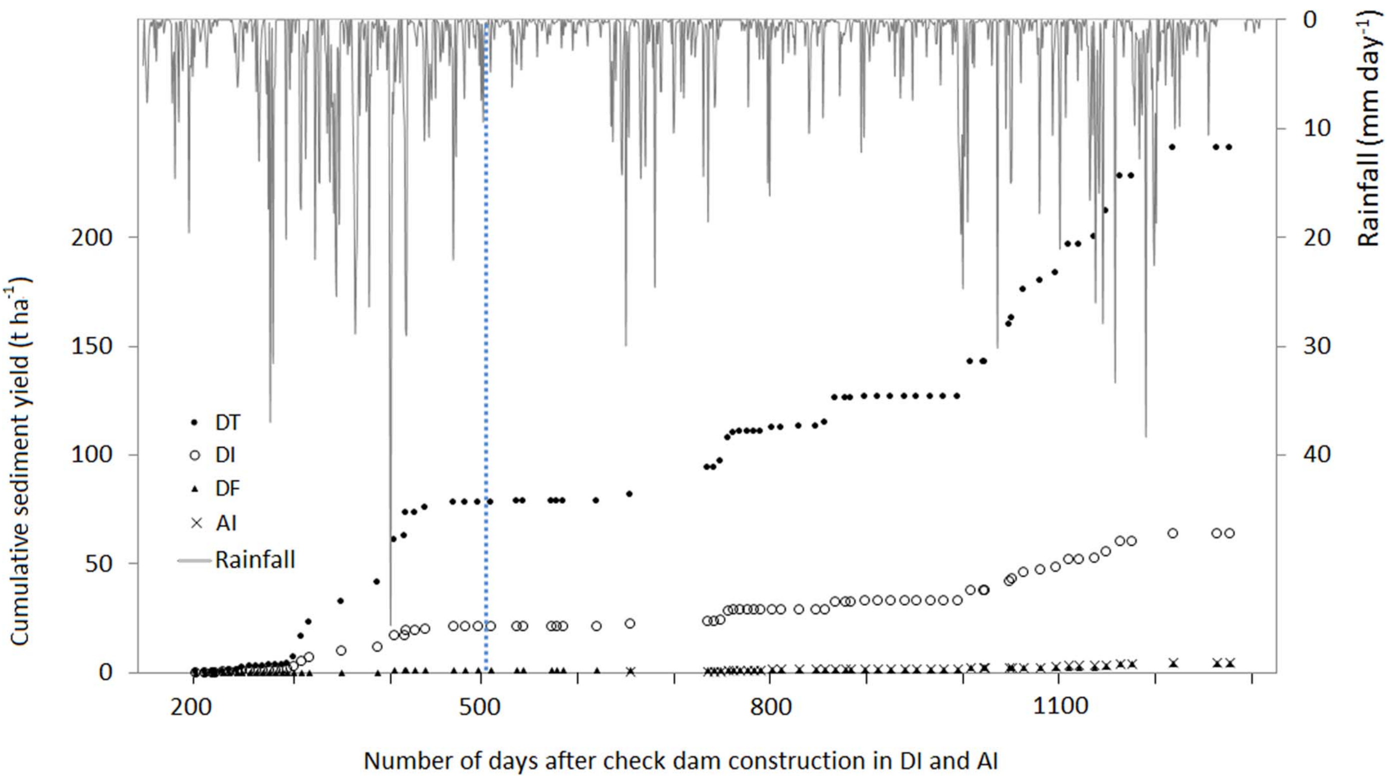

Fig. 7. Cumulative sediment yield of the DT, DI, DF and AI micro-catchments as a function of time, covering the period 01/07/2011–30/07/2014. The vertical dotted line shows the date when all check dams were filled to > 90% of their sediment capacity. In micro-catchment AT, only two events led to (very low amounts of) sediment accumulation in the traps. Daily total rainfall (aggregated from hourly rainfall data) is plotted on the second Y-axis.

The sediment yield of the treated catchment AI is slightly higher than the value measured in the AT micro-catchment, i.e. 2.49 $t\,ha^{-1}\,yr^{-1}$ for AI vs. 0.23 $t\,ha^{-1}\,yr^{-1}$ for AT. This is somewhat unexpected at first sight, and is likely to be the result of differences in land use and management between the two agricultural catchments. Although the total area occupied by agricultural land (arable land and grassland) is rather similar in the two micro-catchments with respectively 82% and 68% of the surface area of AT and AI covered by agricultural land, there is a strong difference in the surface covered by grassland, which is respectively 64% grassland in AT compared to 19% in AI (Table 1, Fig. 3). Previous work by Molina et al. (2008) in the Ecuadorian Andes has shown that the vegetation cover at or near the surface exerts a first order control on erosion rates, explaining 57% of the observed variance in catchment-wide erosion rates. Their empirical erosion model predicts that an increase in vegetation cover of 25% on bare soil leads to a potential reduction in erosion rates by 80% (Molina et al., 2008). As such, the larger area covered by dense grass in the AT micro-catchment has a strong and positive effect on erosion reduction. In the treated agricultural micro-catchment AT, the implementation of check dams caused a net deposition of 591.6 metric tons of eroded material in the gully channels, corresponding to a net deposition rate of 15.7 $t\,ha^{-1}\,yr^{-1}$ (Fig. 8). Our data suggest that about 86% of the sediment that is mobilized within the agricultural AI catchment was trapped behind the check dams, confirming the effectiveness of the flow barriers to trap sediment in the active gully channels.

4. Discussion

The sediment export in the five micro-catchments ranges between 0.23 and 89.1 $t\,ha^{-1}\,yr^{-1}$, with the highest erosion rates observed in the non-treated micro-catchment in eroded land and the lowest rates in agricultural land (Table 2). The magnitude of sediment export and erosion is within the range of those reported under similar soil type, slope and land use conditions by Harden (1993) and Molina et al. (2008). Molina et al. (2008) reported specific sediment yields of 0.26 to 151 $t\,ha^{-1}\,yr^{-1}$ for the Paute river basin, based on field measurements of reservoir infillings (covering 10–40 yr) for catchments of 1 to 296 km^2. The highest sediment yields (> 75 $t\,ha^{-1}\,yr^{-1}$) were observed in dissected badland areas and do not correspond to agricultural land (Vanacker et al., 2007a; Molina et al., 2008). In the central and northern Ecuadorian Andes, soil losses on Andisols averaged 27 $t\,ha^{-1}\,yr^{-1}$ (Henry et al., 2013). In contrast to the southern Ecuadorian Andes, the highest erosion rates were observed in Andisols under annual cropping and tilling (Harden, 1993) with soil losses up to 150 $t\,ha^{-1}\,yr^{-1}$ (Henry et al., 2013) and 836 $t\,ha^{-1}\,yr^{-1}$ (Harden, 1993). Soil crusting and water repellency of Andisols after soil tillage were cited among the major causes of high rates of soil erosion in agricultural land (Poulenard et al., 2001).

The rainfall amount and its intensity control the temporal pattern of sediment mobilization in the micro-catchments. Most of the rainfall events have a low intensity, as only 8% of all rainfall events exceeded 10 $mm\,h^{-1}$ during the monitoring period. Fig. 9 shows the sediment mobilization in the treated micro-catchments DI and AI as a function of the maximum rainfall intensity during 30 min, I_{30max} ($mm\,h^{-1}$). Rainfall events with an $I_{30max} < 10\,mm\,h^{-1}$ do not trigger sediment mobilization in the gully channels indicating that surface runoff, erosion and sediment transport are limited during low intensity rain events. There exists a critical rainfall intensity threshold of 20 to 25 $mm\,h^{-1}$ in the active gully systems: when the rainfall intensity of the event exceeds this threshold, all 45 check dams register sediment filling as they effectively retard the flow of runoff in the gully channel and trigger sediment deposition (Fig. 9). This threshold value is in good agreement with experimental data of rainfall simulation experiments realized in 2004 and 2005 in the Jadan catchment. Fifty-five rainfall simulation experiments using a portable rainfall simulator (effective rainfall intensity of 41 ± 6 $mm\,h^{-1}$) allowed us to establish the cumulative infiltration coefficients for four land use types: eroded land, permanent grassland, arable land and abandoned arable land. Cumulative

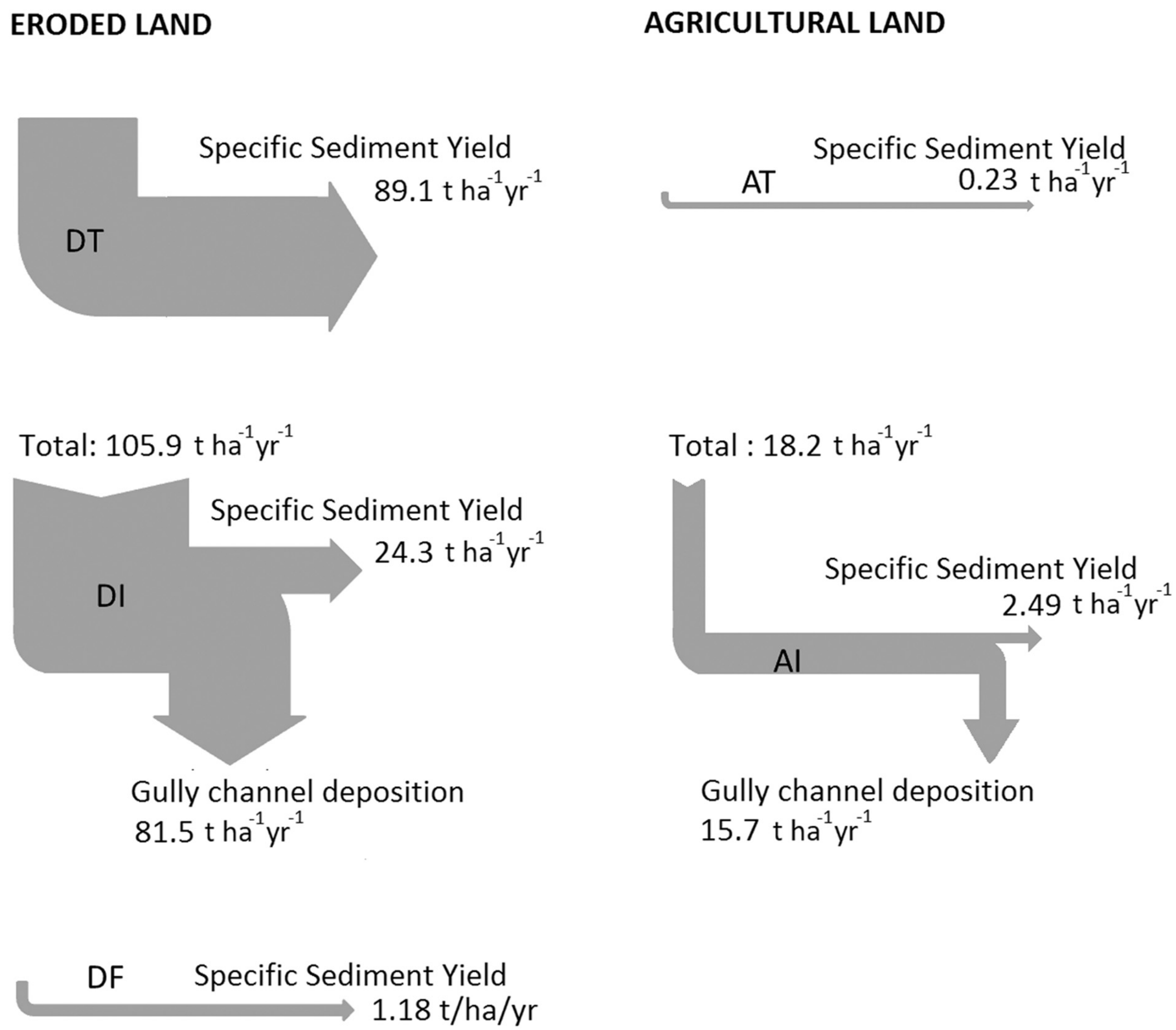

Fig. 8. Simplified sediment budget for the five micro-catchments, highlighting the efficiency of soil and water conservation treatments in reducing the sediment yield at the outlet of the micro-catchments.

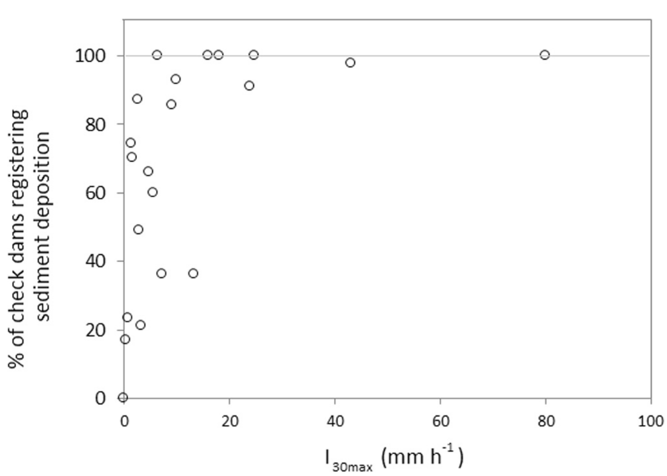

Fig. 9. Percentage of the check dams that registered sediment accumulation during or shortly after a rainfall event with a given rainfall intensity (X-axis). A value of 100% means that for a determined I_{30max}, all the check dams registered sediment accumulation.

infiltration coefficients in eroded land are particularly low: based on the 37 experiments on 1 by 1 m^2 plots in eroded land, an infiltration rate of $22 \pm 10\,mm\,h^{-1}$ was established (Molina et al., 2007). The infiltration rates are strongly controlled by the vegetation cover of the experimental plot. In the absence of a protective vegetation cover, the presence of swelling 2:1 clays leads to rapid sealing and crusting of the soil surface that prevents further infiltration of rain water and gives way to rapid generation of infiltration excess overland flow (Molina et al., 2007).

Soil and water conservation measures have a long-term impact on sediment mobilization and export in the eroded catchments. In eroded land, the implementation of check dams and afforestation reduce the sediment yield from $89.1\,t\,ha^{-1}\,yr^{-1}$ to respectively 24.3 and $1.18\,t\,ha^{-1}\,yr^{-1}$. In contrast to earlier findings by Taye et al. (2015), the effectiveness of the check dams remained constant over time, even after the check dams were filled to about 90 to 100% of their capacity (Fig. 4, Fig. 7). The correlation between the event-based specific sediment yield from the DI and DT micro-catchments is only slightly lower ($R^2 = 0.91$) for the period after filling of check dams compared to the period during which the check dams were capturing sediment ($R^2 = 0.97$). The check dams lowered the channel gradient from > 15% to about 2%, and reduced the flow velocity in the gully channel. Field observations indicated that sediment deposits behind the check dams triggered the growth of pioneer plants in the gully channel. The dense root systems of the pioneer species contributed to stabilize the gully channels, as the vegetation acted as a barrier in flow paths and further reduced the water velocity and enhanced deposition of eroded material.

Our data confirm earlier work by Rey (2004) and Rey and Burylo (2014) that vegetation barriers in gully channels can be very effective in trapping sediment. The combined effect of check dams and spontaneous vegetation succession on young sediment deposits enhances the long-term effectiveness of the erosion restoration programme.

5. Conclusions

Our data show that soil and water conservation treatments such as vegetation restoration and construction of flow barriers in gully systems are very effective in reducing sediment transport in gully systems. The flow barriers that were built in active gully systems are effective in trapping sediment and significantly reduce the sediment export to the fluvial systems: in the eroded and agricultural micro-catchments, about 77% and 86% of the eroded material is trapped in the flow barriers and not exported to the fluvial network. Besides, forestation of active gully systems with rapidly growing exotic species such as *Eucalyptus globulus* has a very positive effect on the stabilization and restoration of the badlands, and effectively reduces the sediment export. Rainfall intensity controls spatio-temporal sediment yield patterns: a critical rainfall threshold of 20 to 25 $mm\,h^{-1}$ exists above which check dams are effectively retarding flow of runoff water and enhancing sediment deposition in the gully channels.

Acknowledgements

The soil restoration project was supported by CGPaute (now SenAgua), ETAPA-DG, EMAC and the Universidad de Cuenca (Ecuador) through the interuniversity project on 'Strengthening the scientific and technological capacities to implement spatially integrated land and water management schemes adapted to local socio-economic and physical settings'. The Académie de Recherche et d'Enseignement Supérieur (ARES) financially supported this project through its Development Cooperation programme (ARES PRD). The authors thank EMAC for the logistical support and facilitation of experimental sites, and the local community of Santa Ana for access to the field sites. A. Molina (No. 20130107) and V. Vanacker (No. 20140615) were supported by Prometeo grants, funded by the Secretaría de Educación Superior de Ciencia, Tecnología e Innovación de la República del Ecuador; and P. Borja by a SENESCYT PhD scholarship (Convocatoria Abierta 2013). The authors thank Dario Alvarado, Charles Bielders, Pedro Cisneros, Marie Guns, Gustavo Tenorio, Bas Van Wesemael and Raul Vanegas for insightful discussions, and Marco Bravin for the assistance with the selection and calibration of field equipment and laboratory analysis. We extend our appreciation to two anonymous reviewers who have provided constructive reviews of the paper.

References

Bellin, N., Vanacker, V., van Wesemael, B., Solé-Benet, A., Bakker, M.M., 2011. Natural and anthropogenic controls on soil erosion in the Internal Betic Cordillera (southeast Spain). Catena 87, 190–200.
Bochet, E., Rubio, J., Poesen, J., 1998. Relative efficiency of three representative matorral species in reducing water erosion at the microscale in a semi-arid climate (Valencia, Spain). Geomorphology 23, 139–150.
Bochet, E., Poesen, J., Rubio, J.L., 2006. Runoff and soil loss under individual plants of a semi-arid Mediterranean shrubland: influence of plant morphology and rainfall intensity. Earth Surf. Process. Landf. 31, 536–549.
Boix-Fayos, C., de Vente, J., Martínez-Mena, M., Barberá, G.G., Castillo, V., 2008. The impact of land use change and check-dams on catchment sediment yield. Hydrol. Process. 22, 4922–4935.
Bruijnzeel, L.A., 2004. Hydrological functions of tropical forests: not seeing the soil for the trees? Agric. Ecosyst. Environ. 104, 185–228.
Burylo, M., Rey, F., Delcros, P., 2007. Abiotic and biotic factors influencing the early stages of vegetation colonization in restored marly gullies (Southern Alps, France). Ecol. Eng. 30, 231–239.
Cadilhac, L., Torres, R., Calles, J., Vanacker, V., Calderon, E., 2017. Desafios para la investigación sobre el cambio climático en Ecuador. Neotrop. Biodivers. 3, 168–181.
Celleri, R., Willems, P., Buytaert, W., Feyen, J., 2007. Space–time rainfall variability in the Paute basin, Ecuadorian Andes. Hydrol. Process. 21, 3316–3327.
Chazdon, R.L., 2008. Beyond deforestation: restoring forests and ecosystem services on degraded lands. Science 320, 1458–1460.
Chirino, E., Bonet, A., Bellot, J., Sánchez, J.R., 2006. Effects of 30-year-old Aleppo pine plantations on runoff, soil erosion, and plant diversity in a semi-arid landscape in south eastern Spain. Catena 65, 19–29.
Cohen, M., Rey, F., 2005. Dynamiques végétales et érosion hydrique sur les marnes dans les Alpes françaises du Sud. Géomorphologie Relief Process. Environ. 31–44.
De Baets, S., Poesen, J., Gyssels, G., Knapen, A., 2006. Effects of grass roots on the erodibility of topsoils during concentrated flow. Geomorphology 76, 54–67.
De Baets, S., Meersmans, J., Vanacker, V., Quine, T.A., Van Oost, K., 2013. Spatial variability and change in soil organic carbon stocks in response to recovery following land abandonment and erosion in mountainous drylands. Soil Use Manag. 29, 65–76.
De Groot, R.S., Blignaut, J., Van Der Ploeg, S., Aronson, J., Elmqvist, T., Farley, J., 2013. Benefits of investing in ecosystem restoration: investing in ecosystem restoration. Conserv. Biol. 27, 1286–1293.
Dehn, M., 1995. An evaluation of soil conservation techniques in the Ecuadorian Andes. Mt. Res. Dev. 15, 175–182.
Descheemaeker, K., Nyssen, J., Poesen, J., Raes, D., Haile, M., Muys, B., Deckers, S., 2006. Runoff on slopes with restoring vegetation: a case study from the Tigray highlands, Ethiopia. J. Hydrol. 331, 219–241.
Duan, X., Liu, B., Gu, Z., Rong, L., Feng, D., 2016. Quantifying soil erosion effects on soil productivity in the hot-dry valley, southwestern China. Environ. Earth Sci. 75 (1164).
Erktan, A., Rey, F., 2013. Linking sediment trapping efficiency with morphological traits of Salix tiller barriers on marly gully floors under ecological rehabilitation. Ecol. Eng. 51, 212–220.
Garcia-Ruiz, J.M., Begueria, S., Nadal-Romero, E., Gonzalez-Hidalgo, J.C., Lana-Renault, N., Sanjuan, Y., 2015. A meta-analysis of soil erosion rates across the world. Geomorphology 239, 160–173.
Google earth V 6.2. (10 January 2008). Quingeo, Ecuador. 2°58'S, 78°56'W. Eye alt 5 km. Digital Globe 2012. http://www.earth.google.com [June, 2012].
Guns, M., Vanacker, V., 2013. Forest cover change trajectories and their impact on landslide occurrence in the tropical Andes. Environ. Earth Sci. 70, 2941–2952.
Gyssels, G., Poesen, J., Bochet, E., Li, Y., 2005. Impact of plant roots on the resistance of soils to erosion by water: a review. Prog. Phys. Geogr. 29, 189–217.
Harden, C., 1988. Mesoscale estimation of soil erosion in the Rio Ambato Drainage, Ecuadorian Sierra. Mt. Res. Dev. 8, 331.
Harden, C.P., 1993. Land use, soil erosion, and reservoir sedimentation in an Andean Drainage Basin in Ecuador. Mt. Res. Dev. 13, 177.
Harden, C., 2001. Soil erosion and sustainable mountain development: experiments, observations and recommendations from the Ecuadorian Andes. Mt. Res. Dev. 21, 77–83.
Harden, C.P., Mathews, L.E., 2002. Hillslope runoff, soil detachment, and soil organic content following reforestation in the Copper Basin, Tennessee, USA. Aust. Geogr. Stud. 40, 130–142.
Harden, C.P., Scruggs, P.D., 2003. Infiltration on mountain slopes: a comparison of three environments. Geomorphology 55, 5–24.
Haregeweyn, N., Tsunekawa, A., Nyssen, J., Poesen, J., Tsubo, M., Meshesha, D.T., Schütt, B., Adgo, E., Tegegne, F., 2015. Soil erosion and conservation in Ethiopia: a review. Prog. Phys. Geogr. 39, 750–774.
Henry, A., Mabit, L., Jaramillo, R.E., Cartagena, Y., Lynch, J.P., 2013. Land use effects on erosion and carbon storage of the Rio Chimbo watershed, Ecuador. Plant Soil 367, 477–491.
Hooke, J., Sandercock, P., 2017. Combating Desertification and Land Degradation. Spatial Strategies Using Vegetation. Springer International Publishing, pp. 135. http://dx.doi.org/10.1007/978-3-319-44451-2.
Imeson, A., 2012. Desertification, Land Degradation and Sustainability. John Wiley & Sons, UK.
Inbar, M., Llerena, C.A., 2000. Erosion processes in high mountain agricultural terraces in Peru. Mt. Res. Dev. 20, 72–79.
IUSS Working Group WRB, 2015. World Reference Base for Soil Resources 2014, Update 2015. International Soil Classification System for Naming Soils and Creating Legends for Soil Maps. World Soil Resources Reports No. 106 FAO, Rome.
Knoke, T., Bendix, J., Pohle, P., Hamer, U., Hildebrandt, P., Roos, K., Gerique, A., Sandoval, M.L., Breuer, L., Tischer, A., Silva, B., Calvas, B., Aguirre, N., Castro, L.M., Windhorst, D., Weber, M., Stimm, B., Günter, S., Palomeque, X., Mora, J., Mosandl, R., Beck, E., 2014. Afforestation or intense pasturing improve the ecological and economic value of abandoned tropical farmlands. Nat. Commun. 5, 5612.
Kosmas, C., Danalatos, N., Cammeraat, L.H., Chabart, M., Gutierrez, L., Jacob, A., Diamantopoulos, J., Farand, R., Marques, H., Mizara, A., Moustakas, N., Nicolau, J.M., Oliveros, C., Pinna, G., Puddu, R., Puigdefabregas, J., Roxo, M., Simao, A., Stamou, G., Tomasi, N., Usai, D., Vacca, A., 1997. The effect of land use on runoff and soil erosion rates under Mediterranean conditions. Catena 29, 45–59.
Marden, M., Herzig, A., Basher, L., 2014. Erosion process contribution to sediment yield before and after the establishment of exotic forest: Waipaoa catchment, New Zealand. Geomorphology 226, 162–174.
Molina, A., Govers, G., Vanacker, V., Poesen, J., Zeelmaekers, E., Cisneros, F., 2007. Runoff generation in a degraded Andean ecosystem: interaction of vegetation cover and land use. Catena 71, 357–370.
Molina, A., Govers, G., Poesen, J., Van Hemelryck, H., De Bièvre, B., Vanacker, V., 2008. Environmental factors controlling spatial variation in sediment yield in a central Andean mountain area. Geomorphology 98, 176–186.
Molina, A., Govers, G., Cisneros, F., Vanacker, V., 2009. Vegetation and topographic controls on sediment deposition and storage on gully beds in a degraded mountain area. Earth Surf. Process. Landf. 34, 755–767.
Molina, A., Vanacker, V., Balthazar, V., Mora, D., Govers, G., 2012. Complex land cover change, water and sediment yield in a degraded Andean environment. J. Hydrol. 472–473, 25–35.

Mora, D.E., Willems, P., 2012. Decadal oscillations in rainfall and air temperature in the Paute River Basin-Southern Andes of Ecuador. Theor. Appl. Climatol. 108, 267–282.
Navarro Hevia, J., de Araujo, J.C., Mongil Manso, J., 2014. Assessment of 80 years of ancient-badlands restoration in Saldaña, Spain. Earth Surf. Process. Landf. 39, 1563–1575.
Pimentel, D., Harvey, C., Resosudarmo, P., Sinclair, K., Kurz, D., McNair, M., Crist, S., Shpritz, L., Fitton, L., Saffouri, R., Blair, R., 1995. Environmental and economic costs of soil erosion and conservation benefits. Science 267, 1117–1123.
Podwojewski, P., Zambrana, T., Poulenard, J., 2002. Overgrazing effects on vegetation cover and properties of volcanic ash soil in the paramo of the Llangahua and Esperanza (Tungurahua, Ecuador). Soil Use Manag. 18, 45–55.
Poesen, J., Nachtergaele, J., Verstraeten, G., Valentin, C., 2003. Gully erosion and environmental change: importance and research needs. Catena 50, 91–133.
Poulenard, J., Podwojewski, P., Janeau, J.-L., Collinet, J., 2001. Runoff and soil erosion under rainfall simulation of Andisols from the Ecuadorian Paramo: effect of tillage and burning. Catena 45, 185–207.
Ramos-Diez, I., Navarro-Hevia, J., San Martín Fernández, R., Díaz-Gutiérrez, V., Mongil-Manso, J., 2016. Analysis of methods to determine the sediment retained by check dams and to estimate erosion rates in badlands. Environ. Monit. Assess. 188, 405.
Rey, F., 2003. Influence of vegetation distribution on sediment yield in forested marly gullies. Catena 50, 549–562.
Rey, F., 2004. Effectiveness of vegetation barriers for marly sediment trapping. Earth Surf. Process. Landf. 29, 1161–1169.
Rey, F., Burylo, M., 2014. Can bioengineering structures made of willow cuttings trap sediment in eroded marly gullies in a Mediterranean mountainous climate? Geomorphology 204, 564–572.
Rey, F., Isselin-Nondedeu, F., Bédécarrats, A., 2005. Vegetation dynamics on sediment deposits upstream of bioengineering works in mountainous marly gullies in a Mediterranean climate (Southern Alps, France). Plant Soil 278, 149–158.
Ruiz Sinoga, J.D., Pariente, S., Diaz, A.R., Martinez Murillo, J.F., 2012. Variability of relationships between soil organic carbon and some soil properties in Mediterranean rangelands under different climatic conditions (South of Spain). Catena 94, 17–25.
Sanders, D., 1988. Soil and water conservation on steep lands: A summary of workshop discussions. In: Moldenhauer, W., Hudson, N. (Eds.), Conservation Farming on Steep Lands. Soil and Water Conservation Society and World Association of Soil and Water Conservation, pp. 275–282.
Sougnez, N., van Wesemael, B., Vanacker, V., 2011. Low erosion rates measured for steep, sparsely vegetated catchments in southeast Spain. Catena 84, 1–11.
Stokes, A., Norris, J., van Beek, L., Bogaard, T., Cammeraat, E., Mickovski, S., Jenner, A., Di Iorio, A., Fourcaud, T., 2008. How vegetation reinforces soil on slopes. In: Norris, J., Stokes, A., Mickovski, S., Cammeraat, E., van Beek, R., Nicoll, B., Achim, A. (Eds.), Slope Stability and Erosion Control: Ecotechnological Solutions. Springer, Dordrecht, pp. 65–117.
Taye, G., Poesen, J., Vanmaercke, M., van Wesemael, B., Martens, L., Teka, D., Nyssen, J., Deckers, J., Vanacker, V., Haregeweyn, N., Hallet, V., 2015. Evolution of the effectiveness of stone bunds and trenches in reducing runoff and soil loss in the semi-arid Ethiopian highlands. Z. Für Geomorphol. 59, 477–493.
Thornes, J.B., 1990. Vegetation and Erosion: Processes and Environments. John Wiley & Sons Ltd, Chichester.
Vanacker, V., Govers, G., Barros, S., Poesen, J., Deckers, J., 2003. The effect of short-term socio-economic and demographic change on landuse dynamics and its corresponding geomorphic response with relation to water erosion in a tropical mountainous catchment, Ecuador. Landsc. Ecol. 18, 1–15.
Vanacker, V., Molina, A., Govers, G., Poesen, J., Deckers, J., 2007a. Spatial variation of suspended sediment concentrations in a tropical Andean river system: the Paute River, southern Ecuador. Geomorphology 87, 53–67.
Vanacker, V., von Blanckenburg, F., Govers, G., Molina, A., Poesen, J., Deckers, J., Kubik, P., 2007b. Restoring dense vegetation can slow mountain erosion to near natural benchmark levels. Geology 35, 303–306.
Verstraeten, G., Bazoffi, P., Lajczak, A., Radoane, M., Rey, F., de Vente, J., 2006. Reservoir and pond sedimentation in Europe. In: Poesen, J., Boardman, J. (Eds.), Soil Erosion in Europe. John Wiley & Sons, Chichester, pp. 759–774.
Xiang-Zhou, X., Hong-wu, Z., Ouyang, Z., 2004. Development of check-dam systems in gullies on the Loess Plateau, China. Environ. Sci. Pol. 7, 79–86.
Xu, X.-L., Ma, K.-M., Fu, B.-J., Song, C.-J., Liu, W., 2008. Influence of three plant species with different morphologies on water runoff and soil loss in a dry-warm river valley, SW China. For. Ecol. Manag. 256, 656–663.
Yang, D., Kanae, S., Oki, T., Koike, T., Musiake, K., 2003. Global potential soil erosion with reference to land use and climate changes. Hydrol. Process. 17, 2913–2928.
Yüksek, T., Yüksek, F., 2011. The effects of restoration on soil properties in degraded land in the semi-arid region of Turkey. Catena 84, 47–53.
Zheng, F., 2006. Effect of vegetation changes on soil erosion on the Loess Plateau. Pedosphere 420–427.